Heme induces autophagic cell death via ER stress in neuron

Zhao Yang (yangzhao5140@sohu.com)
Universitatsklinikum Zentrum fur Neurologie

ZhongYan Huang
Universitatsklinikum Munster Klinik fur Neurologie mit Institut fur Translationale Neurologie

Bing Tang
Universitatsklinikum Munster Klinik fur Neurologie mit Institut fur Translationale Neurologie

Nan Zhang
NEUROLOGY

Na Ji
Universitatsklinikum Munster Klinik fur Neurologie mit Institut fur Translationale Neurologie

Research

Keywords: Heme, autophagic death, ER stress, neuron

Posted Date: December 23rd, 2019

DOI: https://doi.org/10.21203/rs.2.19441/v1

Abstract

Aims Intracerebral hemorrhage (ICH) is serious medical problem and the effective treatment is limited. Hemorrhaged blood is highly toxic to the brain, and heme mainly released from hemoglobin plays a vital role in neurotoxicity. However, the specific mechanism involved in heme mediated neurotoxicity has not been well studied.

Methods In this study, we investigated the neurotoxicity of heme in neurons. Neurons were administrated with heme, and the cell death, autophagy and ER stress were analyzed. In addition, the relationship between autophagy and apoptosis in heme-induced cell death and the downstream effects were also detected.

Results We showed that heme induced cell death and autophagy in neurons. The suppression of autophagy using either pharmacologic inhibitors (3-methyladenine) or RNA interference in essential autophagy genes (BECN1 and ATG5) decreased the cell death induced by heme in neurons. Moreover, ER stress activator thapsigargin increased the cell autophagy and cell death ratio following heme treatment. Autophagy promotes cell apoptosis and cell death induced by heme through BECN1/ ATG5 pathway.

Conclusions Our findings suggest that heme potentiates neuron autophagy via ER stress, in turn inducing cell death via BECN1/ATG5 pathway. Targeting ER stress mediated autophagy might be a promising therapeutic strategy for ICH.

Introduction

Intracerebral hemorrhage (ICH) accounts for 10%-15% of all strokes, and causes severe disability and mortality [1, 2, 3]. During ICH, large numbers of erythrocytes are released into the extracellular spaces in the brain. Following erythrocytes are lysed, extracellular hemoglobin is rapidly oxidized into methemoglobin and releases heme [4, 5]. The free heme binds to lipids intercalating into cell membranes, leading to neuron damage [6, 7, 8].

Autophagy is a fundamental biological process that endows eukaryotic cells with the ability to autodigest portions of their own cytoplasm [9, 10, 11]. Autophagy protects cells against adverse conditions and plays important roles in aging, development, death and apoptosis [12, 13, 14]. Autophagy activation may contribute to ICH induced brain injury[15, 16, 17].

The endoplasmic reticulum (ER) is an intracellular organelle that contributes to membrane biosynthesis and the maintenance of intracellular organizational homeostasis[18, 19, 20]. Numerous studies demonstrate that ER stress plays an important role in many diseases, including hemorrhage stroke, other inflammatory and metabolic diseases[21, 22, 23]. In addition, emerging evidence suggests that ER stress can trigger autophagy[24, 25, 26].

However, the potential of heme to regulate ER stress and the regulation of autophagy on neuron is still unknown. Therefore, in the current study, we propose a hypothesis whether heme could induce ER stress in neurons and contribute to autophagic cell death.

Materials And Methods

Primary cell cultures

Cortical neuronal cultures were prepared from whole cerebral cortices of C57BL/6 mouse embryos (E16). Brain tissue was diced into small fragments and incubated in 0.25% trypsin and 200 μg/ml DNase I in PBS. The suspension was then filtered and centrifuged. The pellet was resuspended in PBS and recentrifuged, and after a final wash in feeding medium, the cells were plated into T75 flasks coated with polyornithine (10 μg/ml). The plating density was 80 million cells in 25 ml of medium. To obtain neuron-enriched cultures, cells in the flasks were treated with at least three cycles of 25 μM cytosine arabinoside (2 d on, 3 d off) to kill dividing astrocytes. The feeding medium during this time was minimum essential medium supplemented with 10% fetal bovine serum, nonessential amino acids, 1 mM sodium pyruvate, 2 mM glutamine, and 10% dextrose. All culture medium supplies were from Invitrogen (Burlington, Ontario, Canada). The resulting cells after three cycles of cytosine arabinoside treatment were neurons in excess of 90% purity, with astrocytes, microglia, and precursor cells forming the rest. The neuron-enriched cultures were retrypsinized and plated at 100,000 cells/well in 16-well Lab-tek slides (Nunc, Naperville, IL) in the above medium. Purity of neuronal cultures was> 95% as confirmed by random staining with neuronal and glia markers. 5 days after plating, neurons had developed a dense network of extensions.

Antibodies and reagents

The adenovirus of the GFP-LC3B fusion protein (C3007) was obtained from Beyotime Institute of Biotechnology. Some chemical reagents were purchased from Sigma, including 3-methyladenine (3-MA, M9281), bafilomycin A1 (Baf A1, B1793), thapsigargin (Thap, T9033), AO (A8097), MDC (30432) and carbobenzoxy-valyl-alanyl-aspartyl- [O-met hyl]- fluoromethyl ketone (Z-VAD-FMK, V116); antibodies against autophagy-related protein 5 (ATG5, WH0009140m1), and MAP1LC3B (L7543), were also obtained from Sigma. The antibody against beclin1 (BECN1, 612112) and ACTA (10731) was obtained from BD Transduction Laboratories and Santa Cruz Biotechnology. Other antibodies against poly(ADP-ribose) polymerase 1 (PARP1, 9542), p-EIF2S1 (9721), ATF4 (11815) and DDIT3 (3087) were obtained from Cell Signaling Technology.

Cell culture

Neurons were cultured in Earle's minimal essential medium (Sigma, M0275) containing 10% fetal bovine serum (Gibco, #10099-141) and 100 U/mL penicillin/streptomycin (Thermo Scientific, #15140148) in a

5% CO_2 incubator at 37 °C. Neurons were treated with either vehicle or hemin (100 μM; Sigma, St. Louis, MO, USA) for 0~6 hs.

Transmission electron microscopy

Neurons were collected and fixed in a solution containing 2.5% glutaraldehyde in 0.1 M sodium cacodylate for 2 hrs, postfixed with 1% OsO4 for 1.5 hrs, washed and stained in 3% aqueous uranyl acetate for 1h. The samples were then washed again, dehydrated with a graded alcohol series, and embedded in Epon-Araldite resin (Canemco, #034). Ultrathin sections were cut on a Reichert ultramicrotome, counterstained with 0.3% lead citrate and examined on a Philips EM420 electron microscope.

GFP-LC3 puncta formation assays

Neurons were infected with GFP-LC3B adenovirus (MOI=100:1) for 24 hs, then cultured with either vehicle or hemin (100 μM) for 24 hs, and fixed in 4% paraformaldehyde for 10 minutes at 37 °C. Confocal microscopy was performed with a Radiance 2000 laser scanning confocal microscope (Bio-Rad, San Francisco, CA), followed by image analysis with LaserSharp 2000 software (Bio-Rad, San Francisco, CA). Images were acquired in a sequential scanning mode. According to methods for monitoring GFP-LC3 puncta formation assays, the average number of MAP1LC3B puncta per cell in GFP-MAP1LC3B-positive cells was determined.

Western blot analysis

Cell medium was removed and plates were washed three times with chilled PBS. The cells were quickly scraped and collected by centrifugation at 4°C, then stored at -80°C. Cell samples were sonicated with Western blot lysis buffer. Protein concentration was determined using a Bio-Rad protein assay kit (Hercules, CA, USA). A 15 μg portion of protein from each sample was separated by sodium dodecyl sulfate-polyacrylamide gel electrophoresis and transferred to a hybond-C-pure nitrocellulose membrane (Amersham, Piscataway, NJ, USA). Membranes were blocked in Carnation nonfat milk and probed with the primary and secondary antibodies. Rabbit polyclonal antibody was used at a 1:1000 dilution (Cappel, MP Biomedicals Inc., OH, U.S.A). Detection was accomplished with goat anti-rabbit IgG (Bio-Rad, Hercules, CA, USA; 1:2500 dilution). The antigen-antibody complexes were observed with the ECL chemiluminescence system (Amersham, Piscataway, NJ, USA). Membranes were stripped and reprobed with antibody against actin (Sigma, St Louis, MO, USA; 1:6000 dilution). The relative densities of bands were analyzed with the NIH Image (Version 1.61).

Cell viability

According to the manufacturer's instructions (Sigma), Cell viability was determined with an MTT assay. Following treatment, neurons were incubated with MTT at a final concentration of 5 mg/L for 2 hours and then dissolved in the MTT solubilization solution. The cell survival rate was measured with an absorbance at 590 nm (A590) by a microplate reader (Bio-Rad).

Cell death assay

Cell death was assessed using a PI staining assay. The cells were trypsinized, collected, and resuspended in 2 ml of PBS, then incubated with the PI staining solution at 37 °C for 30 min in the dark before being finally measured with flow cytometry.

Apoptosis

The ratio of apoptotic cells was evaluated by staining 5×10^5 cells with an ANXA5/annexin V-FITC/PI Detection Kit (Invitrogen, V13242) according to the manufacturer's protocol. The samples were analyzed by flow cytometry (BD FACScan Flow cytometer, United States) to determine the percentage of cells displaying annexin V^+/PI^- (early apoptosis) or annexin V^+/PI^+ staining (late apoptosis). For each sample, we report the percentage values corresponding to annexin V-FITC positive cells. Three independent experiments were performed for each assay condition.

Acridine orange staining

In acridine orange-stained cells, the cytoplasm and nucleus appear bright green and dim red, respectively, and acidic compartments appear bright red. The intensity of the red fluorescence is proportional to the degree of acidity. After receiving the specified treatments, cells were incubated with acridine orange solution (1 mg/ml) for 15 min in drug-free medium at 37 °C and washed with PBS. Then, cells were trypsinised and analysed by flow cytometry using a FACScan cytometer and CellQuest software. Statistical analyses were performed as described above.

Monodansylcadaverine (MDC) staining

Monodansylcadaverine (MDC) staining was used to quantify the induction of autophagy with heme. Following treatment, cells were stained with MDC at a final concentration of 10 mM for 10 min at 37 °C, collected and fixed in 3% paraformaldehyde in phosphate-buffered saline for 30 min. The cells were then trypsinised and analysed by flow cytometry using a FACScan cytometer and CellQuest software. For each condition, the percentage of cells with characteristic punctuate MDC staining indicative of autophagy was assessed.

Statistical analysis

The results are expressed as the mean ± standard error (SEM). Two group data were analyzed by Student's t-test, and multiple group data were analyzed using one-way analysis of variance (ANOVA). Statistically significant differences are indicated by asterisks (*P<0.05).

Results

Heme induced cell death in neurons

To investigate whether heme could induce cell death in neurons, we performed a cell death assay using a PI staining assay. As shown in Fig. 1A, the cell death ratio of heme group was much higher than control groups. However, the cell survival ratio of heme group was much lower than control groups (P<0.05) (Fig. 1B). These data indicate that heme induced cell death in neurons.

Heme induced cell death on autophagy

To investigate whether heme induced cell death in time-dependent manner, we performed a cell death assay at 1h, 6hs or 12hs. As shown in Fig. 2A, there were time-dependent increases in cell death ratio after heme treatment. Similar time-dependent decreases in cell viability ratio were observed in MTT assays (Fig. 2B). These data indicate that heme induces cell death in time-dependent manner. In addition, to further analyze whether autophagy contributed to heme induced cell death, we performed a cell death assay and cell viability after the cells were pretreated with 3-MA. The results demonstrated that autophagy inhibitor 3-MA decreased the cell death ratio, while increased cell viability compared with control groups (P<0.05). In addition, the apoptosis inhibitor Z-VAD had the similar effects (P<0.05) (Fig. 2C-D).

Heme treatment induced cell autophagy

To determine whether heme treatment induced autophagy, we utilized acridine orange staining and MDC staining assays to analyze the number of autophagosomes. The data demonstrated that heme revealed

an increase in the number of autophagosomes (Fig. 3A and 3B). MAP1LC3B (using Actin as a loading control), which is considered an accurate indicator of autophagy. We also observed a gradual increase in the ratio of MAP1LC3B-II to Actin in cells treated with heme compared to control cells after 6 hs (Fig. 3C). Furthermore, Baf A1 challenge resulted in the further accumulation of MAP1LC3B-II in neurons after 6 hrs (Fig. 3D), suggesting that heme promotes cellular autophagic flux. To further investigate that heme induces autophagy in neurons, we used a GFP-MAPLC3B puncta formation assay to monitor autophagy. As shown in Fig. 3E, heme-treated neurons demonstrated a significant increase in the percentage of cells with autophagosomes (GFP-MAPLC3B puncta) compared with control cells. TEM of neurons treated with heme revealed an increase in the number of autophagosomes (Fig. 3F). The results suggest that heme induces a complete autophagic response in neurons.

Heme treatment induced cell autophagy via ER stress

To detect whether heme induced ER stress in neurons, we analyzed the ultrastructure of heme-treated neurons using electron microscopy. The data demonstrated that there was more dilated ERs in the heme treatment group than in the control group ($P < 0.05$) (Fig. 4A). To further analyze the effect of ER stress on antophagy, neurons were pretreated with ER stress activator Thap, and administrated with heme. We observed a gradual increase in the ratio of MAP1LC3B-II to Actin in cells pretreated with Thap compared to control cells after 6 hs (Fig. 4B). In addition, acridine orange staining assay demonstrated that Thap revealed an increase in the number of autophagosomes (Fig. 4C). Furthermore, PI staining assay suggested that ER stress activator Thap increased the cell death ratio following heme treatment (Fig.4D). These data revealed that heme treatment induced cell autophagy via ER stress.

Heme treatment induced ER stress mediated cell autophagy through DDIT3/ATF4 pathway

To detect whether heme induced ER stress in time-dependent manner, we analyzed the ER stress marker p-EIF2S1 of heme-treated neurons by western blot assay. The data demonstrated that heme treatment increased p-EIF2S1 levels from 0h to 12 hrs (Fig. 5A). In addition, we analyzed the number of autophagosomes and cell death ratio of heme-treated neurons. The data demonstrated that heme treatment increased the number of autophagosomes and promoted cell death ratio of neurons from 0h to 12 hrs (Fig. 5C and 5E). To further address the possibility that the inhibition of ER stress is responsible for the cell autophagy induced by heme, we assessed the effects of DDIT3 and ATF4 silencing and autophagy and cell death by RNA interference (Fig. 5B and 5D and 5F). The siRNA- mediated knockdown of DDIT3 and ATF4, which are required for ER stress, decreased heme-induced autophagy and cell death, suggesting that ER stress promotes autophagy and the cell death induced by heme through DDIT3/ATF4 pathway.

Autophagy is upstream of apoptosis in heme-induced cell death

Furthermore, we determined the relationship between autophagy and apoptosis in heme-induced cell death. We utilized acridine orange staining and WB assays to analyze autophagy level. The data demonstrated that 3-MA decreased heme induced neuron autophagy (Fig. 6A and 6B). In addition, 3-MA decreased heme induced capase-3 levels of neurons (Fig. 6C). To further address the possibility that inhibition of autophagy is responsible for the cell apoptosis induced by heme, we assessed the effects of BECN1 and ATG5 silencing and autophagy and cell death by RNA interference (Fig. 6D-F). The siRNA-mediated knockdown of BECN1 and ATG5, which are required for autophagy, decreased heme-induced PARP1 levels and cell death, suggesting that autophagy promotes cell apoptosis and cell death induced by heme through BECN1/ ATG5 pathway. Moreover, we assessed the effects of apoptosis inhibitor Z-VAD on cell autophagy. The results demonstrated that inhibition of cell apoptosis could not decreased cell autophagy levels (Fig. 6G-I). These data revealed that autophagy is upstream of apoptosis in heme-induced cell death.

Discussion

In this study, we firstly represented that heme induces autophagic cell death via ER stress in neurons. The data is supported by the following evidence: (1) heme treatment induced cell autophagy; (2) heme treatment induced cell autophagy via ER stress; (3) heme treatment induced ER stress mediated cell autophagy through DDIT3/ATF4 pathway; and (4) autophagy is upstream of apoptosis in heme-induced cell death.

Intracerebral hemorrhage (ICH) is a common and serious acute cerebrovascular disease, and most of the survivors suffer from apparent disability[27, 28, 29]. Free heme is released during erythrocyte lysis, and then degraded by heme oxygenase to form iron. Accumulation of heme and iron in the perihematoma region is characterized by neurotoxicity, and causes acute inflammation resulting in neurology dysfunction[30, 31]. To investigate the neurotoxicity effect of heme on neurons, we cocultured neurons and heme together, and detected the neuron death and viability. The data indicated that heme increased cell death and decreased cell viability in a time-dependent manner. However, the molecular mechanism of heme mediated neurotoxicity on neurons has not been well reported.

Autophagy is the process of bulk degradation and recycling of long-lived proteins, macromolecular aggregates, and damaged intracellular organelles [32, 33, 34]. Cellular homeostasis requires continuous removal of worn-out components and replacement with newly synthesized proteins. Recent studies have enlarged the knowledge of the molecular mechanism of autophagy and the effect of autophagy in different pathological conditions. Autophagy has been identified in a number of pathological conditions, including cancer, myopathies, and neurodegenerative disorders [35, 36, 37]. Autophagy has also been associated with both cell survival and cell death, but the role of autophagy in cell death has been controversial [38, 39, 40]. Therefore, to further identify whether autophagy could be induced after heme treatment, we investigated the autophagy formation and the specific role in neuron survival or death. We

utilized acridine orange staining and MDC staining assays to analyze the number of autophagosomes, and found that heme induced a complete autophagic response in neurons. In addition, we found that autophagy inhibitor 3-MA decreased the cell death ratio, while increased cell viability.

The endoplasmic reticulum (ER) is an intracellular organelle where the protein molecule folding, transportation, or modification takes place and also a place for calcium storage, lipid synthesis, and carbohydrate metabolism[41, 42, 43]. Much evidences observed that the homeostasis of ER alters under certain pathological conditions leading to the accumulation of misfolded or unfolded proteins and ER stress. Recent evidence reveals that ER stress can stimulate autophagy[44]. However, the role of heme in ER stress-induced autophagy and the related signal events remain to be fully illustrated. We assessed the effects of DDIT3 and ATF4 silencing and autophagy and cell death by RNA interference. We found that knockdown of DDIT3 and ATF4 decreased heme-induced autophagy and cell death, suggesting that ER stress promotes autophagy and the cell death induced by heme through DDIT3/ATF4 pathway.

The interactions between apoptotic and autophagic proteins via the proteolytic systems are known mechanisms through which autophagy and apoptosis regulate each other[45, 46]. Finally, we determined the relationship between autophagy and apoptosis in heme-induced cell death. We found that autophagy promoted cell apoptosis and cell death induced by heme through BECN1/ ATG5 pathway. However, inhibition of cell apoptosis could not decreased cell autophagy levels. These data revealed that autophagy is upstream of apoptosis in heme-induced cell death.

Conclusion

Our findings suggested that heme initiated neuron autophagy via ER stress, in turn inducing cell death via BECN1/ATG5 pathway. Targeting ER stress mediated autophagy might be a promising therapeutic strategy for ICH.

Declarations

Acknowledgements

None.

Authors' contributions

Conceptualization: ZY; Methodology: BT, and NZ; Manuscript Preparation: NJ. All authors read and approved the final manuscript.

Funding

The study was supported by Natural Science Foundation of Yongchuan district of Chongqing (Ycstc, 2017nc5023).

Ethics approval and consent to participate

All animals received care in compliance with the Principles of Laboratory Animal Care and National standards.

Availability of data and materials

Please contact author for data requests.

Consent for publication

Not applicable.

Competing interests

The authors declare that they have no competing interests**.**

References

1. Sennfalt S, Norrving B, Petersson J, Ullberg T (2018) Long-Term Survival and Function After Stroke. Stroke: STROKEAHA118022913.
2. Yu Z, Zheng J, Guo R, Ma L, You C, et al. (2019) Prognostic significance of leukoaraiosis in intracerebral hemorrhage: A meta-analysis. J Neurol Sci 397: 34-41.
3. Khatri R, Afzal MR, Qureshi MA, Maud A, Huanyu D, et al. (2019) Pre-Existing Renal Failure Increases In-Hospital Mortality in Patients with Intracerebral Hemorrhage. J Stroke Cerebrovasc Dis 28: 237-242.
4. Takeuchi S, Kawauchi S, Sato S, Nawashiro H, Nagatani K, et al. (2013) Evaluation of the stage of hemorrhage using optical diffuse reflectance spectroscopy: an in vivo study. Acta Neurochir Suppl 118: 45-48.
5. Chen-Roetling J, Sinanan J, Regan RF (2012) Effect of iron chelators on methemoglobin and thrombin preconditioning. Transl Stroke Res 3: 452-459.
6. Shen J, Liu Y, Song Y, Li L, Duan C, et al. (2015) CHMP4B, ESCRT-III associating protein, associated with neuronal apoptosis following intracerebral hemorrhage. Brain Res 1597: 1-13.
7. Lakovic K, Ai J, D'Abbondanza J, Tariq A, Sabri M, et al. (2014) Bilirubin and its oxidation products damage brain white matter. J Cereb Blood Flow Metab 34: 1837-1847.
8. Caliaperumal J, Wowk S, Jones S, Ma Y, Colbourne F (2013) Bipyridine, an iron chelator, does not lessen intracerebral iron-induced damage or improve outcome after intracerebral hemorrhagic stroke in rats. Transl Stroke Res 4: 719-728.
9. Jin S, Wei J, You L, Liu H, Qian W (2018) Autophagy regulation and its dual role in blood cancers: A novel target for therapeutic development (Review). Oncol Rep 39: 2473-2481.

10. Stavoe AKH, Holzbaur ELF (2019) Axonal autophagy: Mini-review for autophagy in the CNS. Neurosci Lett 697: 17-23.
11. Han Y, Fan S, Qin T, Yang J, Sun Y, et al. (2018) Role of autophagy in breast cancer and breast cancer stem cells (Review). Int J Oncol 52: 1057-1070.
12. Geronimo-Olvera C, Montiel T, Rincon-Heredia R, Castro-Obregon S, Massieu L (2017) Autophagy fails to prevent glucose deprivation/glucose reintroduction-induced neuronal death due to calpain-mediated lysosomal dysfunction in cortical neurons. Cell Death Dis 8: e2911.
13. Galluzzi L, Bravo-San Pedro JM, Demaria S, Formenti SC, Kroemer G (2017) Activating autophagy to potentiate immunogenic chemotherapy and radiation therapy. Nat Rev Clin Oncol 14: 247-258.
14. Marion J, Le Bars R, Besse L, Batoko H, Satiat-Jeunemaitre B (2018) Multiscale and Multimodal Approaches to Study Autophagy in Model Plants. Cells 7.
15. Shi H, Wang J, Huang Z, Yang Z (2018) IL-17A induces autophagy and promotes microglial neuroinflammation through ATG5 and ATG7 in intracerebral hemorrhage. J Neuroimmunol 323: 143-151.
16. Duan XC, Wang W, Feng DX, Yin J, Zuo G, et al. (2017) Roles of autophagy and endoplasmic reticulum stress in intracerebral hemorrhage-induced secondary brain injury in rats. CNS Neurosci Ther 23: 554-566.
17. Shen X, Ma L, Dong W, Wu Q, Gao Y, et al. (2016) Autophagy regulates intracerebral hemorrhage induced neural damage via apoptosis and NF-kappaB pathway. Neurochem Int 96: 100-112.
18. Rieusset J (2018) The role of endoplasmic reticulum-mitochondria contact sites in the control of glucose homeostasis: an update. Cell Death Dis 9: 388.
19. Xue Y, Schmollinger S, Attar N, Campos OA, Vogelauer M, et al. (2017) Endoplasmic reticulum-mitochondria junction is required for iron homeostasis. J Biol Chem 292: 13197-13204.
20. Ushioda R, Miyamoto A, Inoue M, Watanabe S, Okumura M, et al. (2016) Redox-assisted regulation of Ca2+ homeostasis in the endoplasmic reticulum by disulfide reductase ERdj5. Proc Natl Acad Sci U S A 113: E6055-E6063.
21. Niu M, Dai X, Zou W, Yu X, Teng W, et al. (2017) Autophagy, Endoplasmic Reticulum Stress and the Unfolded Protein Response in Intracerebral Hemorrhage. Transl Neurosci 8: 37-48.
22. Duan X, Wen Z, Shen H, Shen M, Chen G (2016) Intracerebral Hemorrhage, Oxidative Stress, and Antioxidant Therapy. Oxid Med Cell Longev 2016: 1203285.
23. Kwon SK, Ahn M, Song HJ, Kang SK, Jung SB, et al. (2015) Nafamostat mesilate attenuates transient focal ischemia/reperfusion-induced brain injury via the inhibition of endoplasmic reticulum stress. Brain Res 1627: 12-20.
24. Roest G, Hesemans E, Welkenhuyzen K, Luyten T, Engedal N, et al. (2018) The ER Stress Inducer l-Azetidine-2-Carboxylic Acid Elevates the Levels of Phospho-eIF2alpha and of LC3-II in a Ca(2+)-Dependent Manner. Cells 7.

25. Lambelet M, Terra LF, Fukaya M, Meyerovich K, Labriola L, et al. (2018) Dysfunctional autophagy following exposure to pro-inflammatory cytokines contributes to pancreatic beta-cell apoptosis. Cell Death Dis 9: 96.
26. Tschurtschenthaler M, Adolph TE, Ashcroft JW, Niederreiter L, Bharti R, et al. (2017) Defective ATG16L1-mediated removal of IRE1alpha drives Crohn's disease-like ileitis. J Exp Med 214: 401-422.
27. Zhang R, Ji R, Pan Y, Jiang Y, Liu G, et al. (2017) External Validation of the Prestroke Independence, Sex, Age, National Institutes of Health Stroke Scale Score for Predicting Pneumonia After Stroke Using Data From the China National Stroke Registry. J Stroke Cerebrovasc Dis 26: 938-943.
28. Sipila JO, Ruuskanen JO, Kauko T, Rautava P, Kyto V (2017) Seasonality of stroke in Finland. Ann Med 49: 310-318.
29. Payabvash S, Noorbaloochi S, Qureshi AI (2017) Topographic Assessment of Acute Ischemic Changes for Prognostication of Anterior Circulation Stroke. J Neuroimaging 27: 227-231.
30. Kwon KJ, Kim JN, Kim MK, Kim SY, Cho KS, et al. (2013) Neuroprotective effects of valproic acid against hemin toxicity: possible involvement of the down-regulation of heme oxygenase-1 by regulating ubiquitin-proteasomal pathway. Neurochem Int 62: 240-250.
31. Zhao X, Grotta J, Gonzales N, Aronowski J (2009) Hematoma resolution as a therapeutic target: the role of microglia/macrophages. Stroke 40: S92-94.
32. Marshall RS, Vierstra RD (2018) Autophagy: The Master of Bulk and Selective Recycling. Annu Rev Plant Biol 69: 173-208.
33. Elander PH, Minina EA, Bozhkov PV (2018) Autophagy in turnover of lipid stores: trans-kingdom comparison. J Exp Bot 69: 1301-1311.
34. Wu MY, Song JX, Wang SF, Cai CZ, Li M, et al. (2018) Selective autophagy: The new player in the fight against neurodegenerative diseases? Brain Res Bull 137: 79-90.
35. Chen Y, Scarcelli V, Legouis R (2017) Approaches for Studying Autophagy in Caenorhabditis elegans. Cells 6.
36. Benito-Cuesta I, Diez H, Ordonez L, Wandosell F (2017) Assessment of Autophagy in Neurons and Brain Tissue. Cells 6.
37. Conte A, Paladino S, Bianco G, Fasano D, Gerlini R, et al. (2017) High mobility group A1 protein modulates autophagy in cancer cells. Cell Death Differ 24: 1948-1962.
38. Nazim UM, Jeong JK, Seol JW, Hur J, Eo SK, et al. (2015) Inhibition of the autophagy flux by gingerol enhances TRAIL-induced tumor cell death. Oncol Rep 33: 2331-2336.
39. Lalaoui N, Lindqvist LM, Sandow JJ, Ekert PG (2015) The molecular relationships between apoptosis, autophagy and necroptosis. Semin Cell Dev Biol 39: 63-69.
40. Tian Y, Kuo CF, Sir D, Wang L, Govindarajan S, et al. (2015) Autophagy inhibits oxidative stress and tumor suppressors to exert its dual effect on hepatocarcinogenesis. Cell Death Differ 22: 1025-1034.
41. Yi MC, Melkonian AV, Ousey JA, Khosla C (2018) Endoplasmic reticulum-resident protein 57 (ERp57) oxidatively inactivates human transglutaminase 2. J Biol Chem 293: 2640-2649.

42. Ishikawa Y, Holden P, Bachinger HP (2017) Heat shock protein 47 and 65-kDa FK506-binding protein weakly but synergistically interact during collagen folding in the endoplasmic reticulum. J Biol Chem 292: 17216-17224.
43. Obakan-Yerlikaya P, Arisan ED, Coker-Gurkan A, Adacan K, Ozbey U, et al. (2017) Calreticulin is a fine tuning molecule in epibrassinolide-induced apoptosis through activating endoplasmic reticulum stress in colon cancer cells. Mol Carcinog 56: 1603-1619.
44. Bao Y, Pu Y, Yu X, Gregory BD, Srivastava R, et al. (2018) IRE1B degrades RNAs encoding proteins that interfere with the induction of autophagy by ER stress in Arabidopsis thaliana. Autophagy 14: 1562-1573.
45. Warri A, Cook KL, Hu R, Jin L, Zwart A, et al. (2018) Autophagy and unfolded protein response (UPR) regulate mammary gland involution by restraining apoptosis-driven irreversible changes. Cell Death Discov 4: 40.
46. Yuan Y, Ding D, Zhang N, Xia Z, Wang J, et al. (2018) TNF-alpha induces autophagy through ERK1/2 pathway to regulate apoptosis in neonatal necrotizing enterocolitis model cells IEC-6. Cell Cycle 17: 1390-1402.

Figures

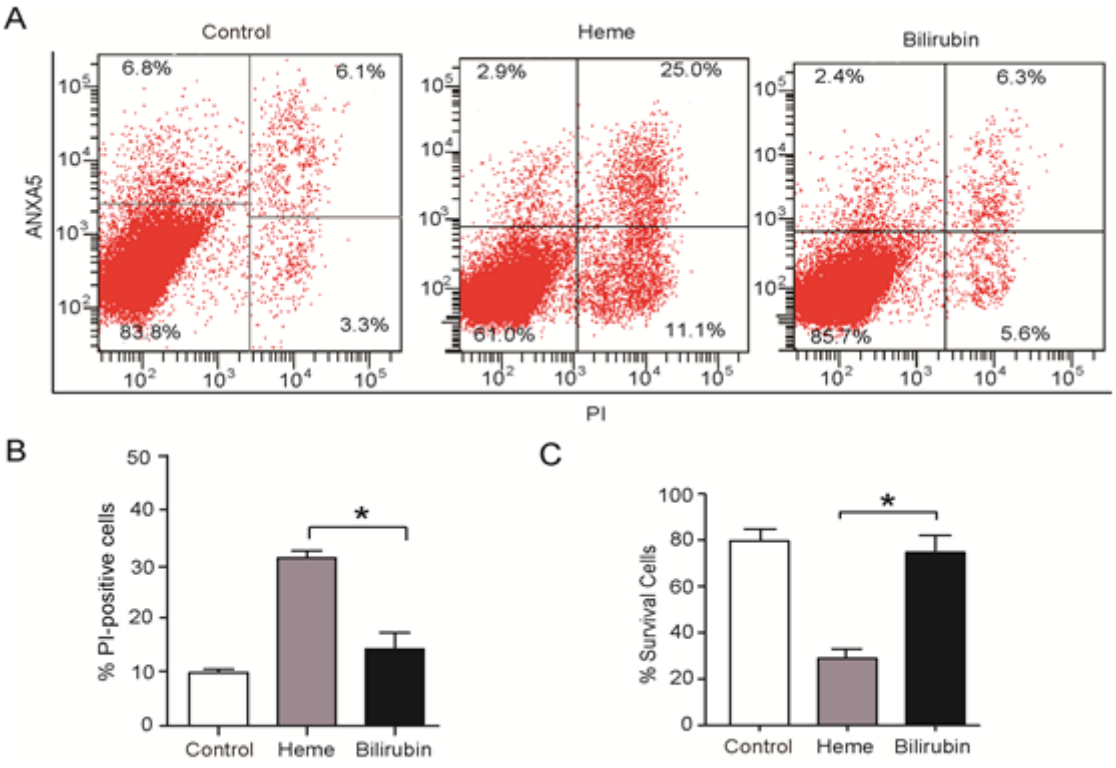

Figure 1

Heme induced cell death in neurons. To assess cell death in vitro, neurons with the treated with heme for 6 hrs, and analyzed by flow cytometry with annexin V/PI staining. (A) The represent FACS data of different groups. (B) The PI positive cells of different groups. (C) The survival cell ratio of different groups. Experiments performed in triplicate showed consistent results. Data are presented as the mean ± SD of three independent experiments. * P<0.05.

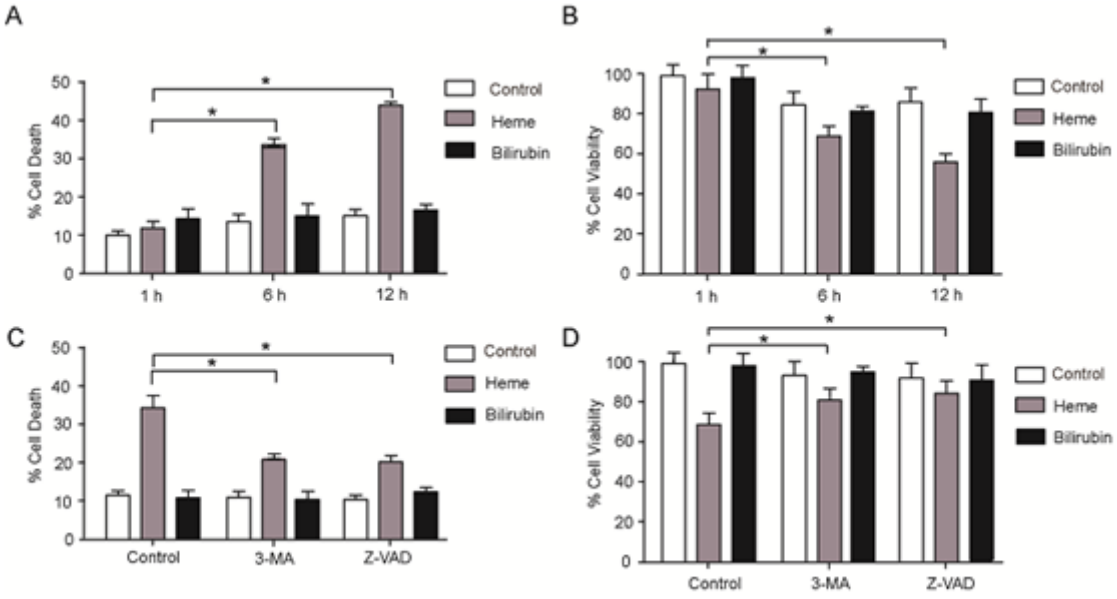

Figure 2

Heme induced cell death on autophagy (A) To assess cell death in vitro, neurons with the treatment for the indicated time were subjected to PI staining, and analyzed by flow cytometry. The percentage of cells with PI-positive relative to total cell number at each treatment is shown. (B) The effect of heme on the viability of neurons. Neurons were treated with the indicated time. Cell viability was assessed using MTT. (C) To assess cell death in vitro, neurons with the treatment for 6 hrs were subjected to PI staining, and analyzed by flow cytometry. The percentage of cells with PI-positive relative to total cell number at each treatment is shown. (D) The effect of heme on the viability of neurons. Neurons were treated with 3-MA or controls for 6 hrs. Cell viability was assessed using MTT. Data are presented as the mean ± SD of three independent experiments. * P<0.05.

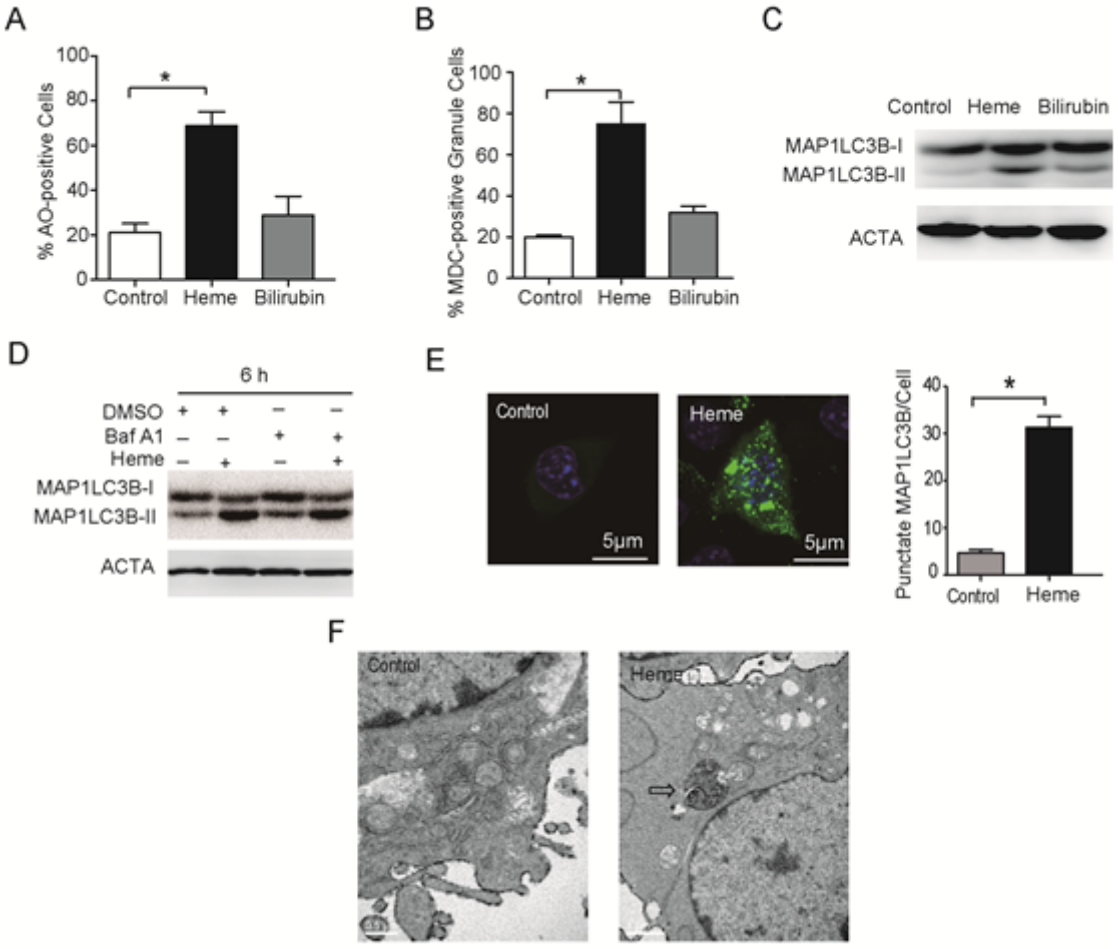

Figure 3

Heme treatment induced cell autophagy (A and B) Neurons were treated with heme or controls for 6 hrs and stained with 1 mg/ml acridine orange or 50 mM MDC for 15 mins. After incubation, cells were immediately analysed by flow cytometry. The bar chart demonstrates an increase in mean fluorescent intensity. The asterisks denote significant differences from controls. (C) Neurons were treated with heme for 6 hrs, and MAP1LC3B-II levels were analyzed. (D) Heme induced complete autophagic flux in neurons. Neurons were treated with heme or control for in the presence or absence of Baf A1 (10 nM). (E) Neurons were transfected with GFP-LC3B adenovirus. After 24 hrs, the cells were exposed to heme for 6 hrs. Cells were visualised by confocal microscopy immediately after fixation. The number of GFP-LC3B puncta in each cell was counted. (F) Ultrastructural changes in heme-treated neurons. The control shows samples without heme treatment. Closed arrows indicate autophagosomes. Data are presented as the mean ± SD of three independent experiments. * $P<0.05$.

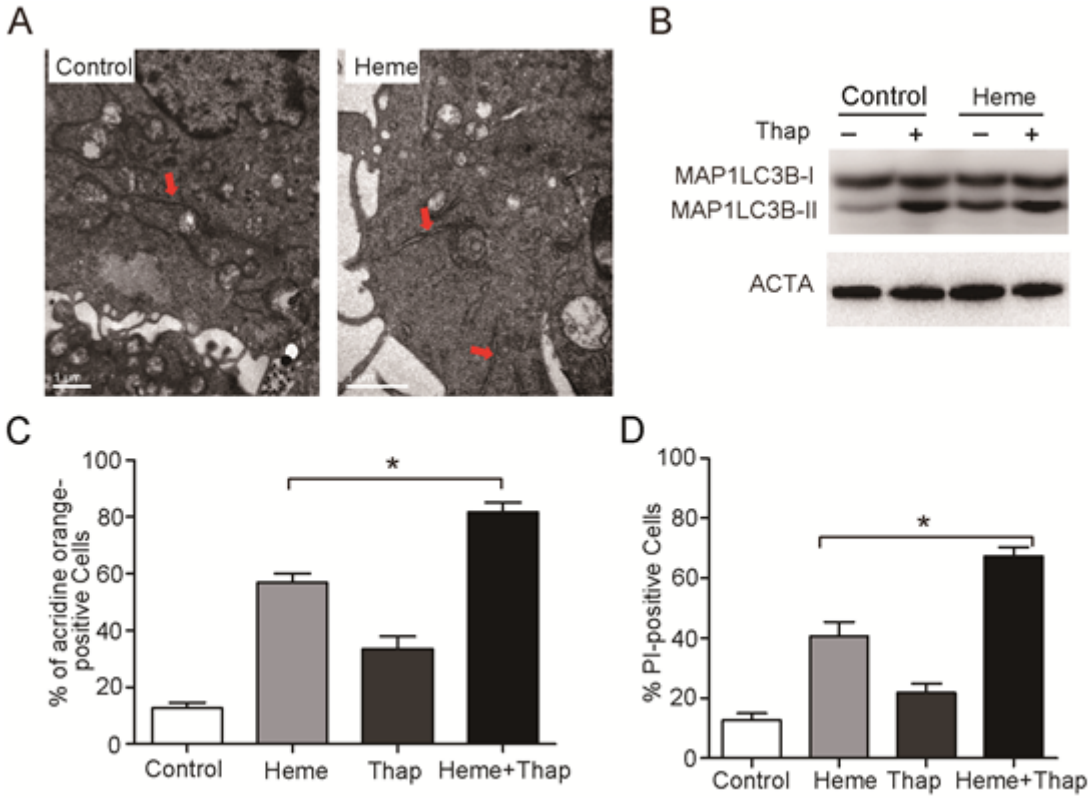

Figure 4

Heme treatment induced cell autophagy via ER stress (A) Neurons (1×105) were stimulated with control, or heme for 6 hrs. After that, neurons were directly fixed with 1% glutaraldehyde and postfixed with 2% osmium tetraoxide. The dilatation of the ER was observed with arrows. (B) Neurons (1×105) were stimulated with control, or heme in the presence or absence of Thap for 6 hrs, and MAP1LC3B-II levels were analyzed. (C) Neurons (1×105) were stimulated with control, or heme in the presence or absence of Thap for 6 hrs, and stained with 1 mg/ml acridine for 15 min. After incubation, cells were immediately analysed by flow cytometry. (D) Neurons (1×105) were stimulated with control, or heme in the presence or absence of Thap for 6 hrs, and were subjected to PI staining, and analyzed by flow cytometry. Data are presented as the mean ± SD of three independent experiments. * $P<0.05$.

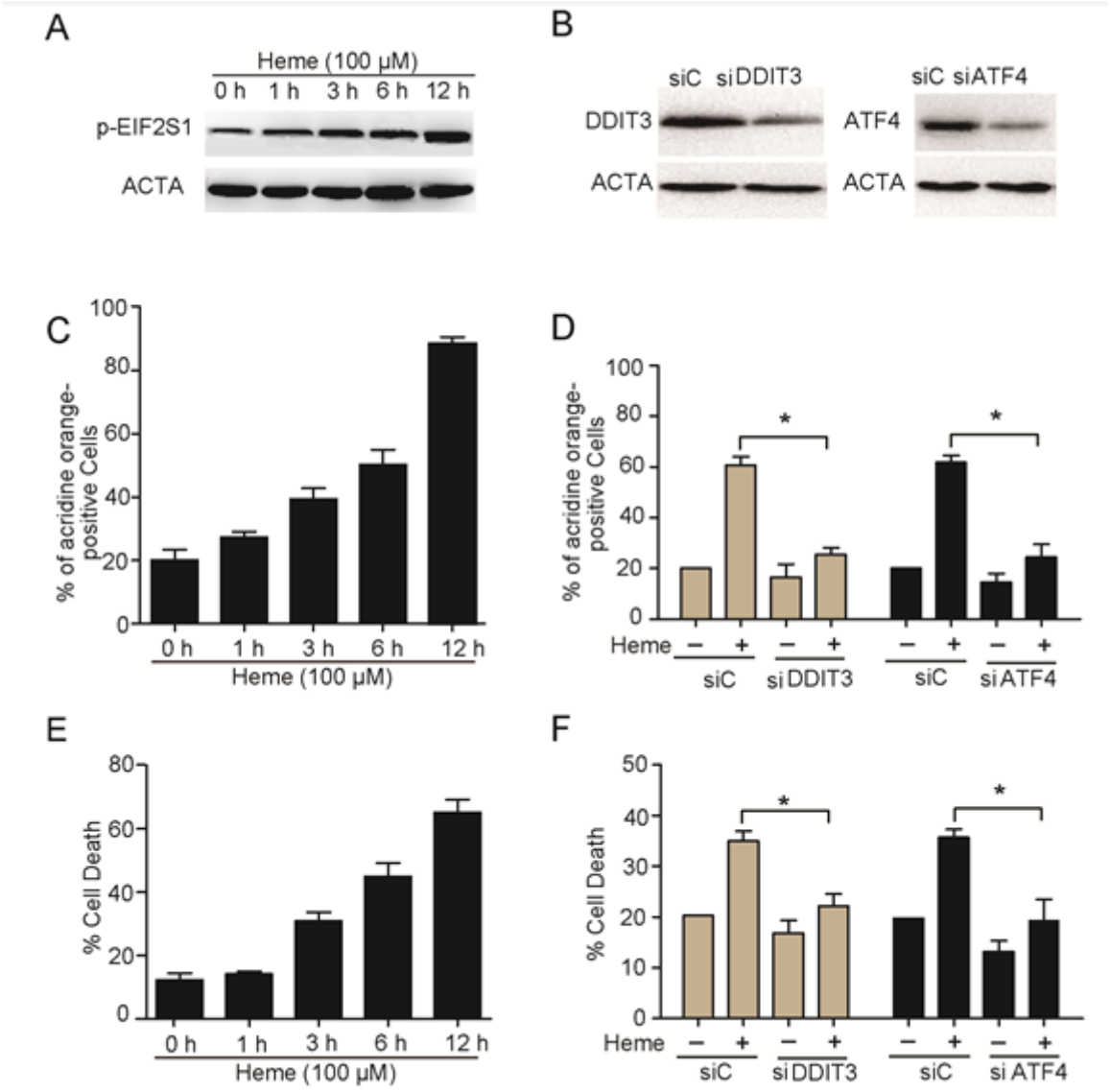

Figure 5

Heme treatment induced ER stress mediated cell autophagy through DDIT3/ATF4 pathway (A) Neurons (1×105) were stimulated with heme for indicated time, and cells were analyzed for p-EIF2S1 levels. (B) Detection of the inhibition efficiency of siRNAs against DDIT3 and ATF4. Neurons were transfected with siRNAs targeting DDIT3 or ATF4 (100 nM each) for 24 hrs, and the protein levels of the target were evaluated by Western blotting. (C) Neurons (1×105) were stimulated with heme for indicated time, and stained with 1 mg/ml acridine for 15 mins. After incubation, cells were immediately analysed by flow cytometry. (D) Neurons were tranduced with DDIT3 RNAi or ATF4 RNAi for 24 hrs, and were further stimulated with control or heme for 6 hrs. Cells were stained with 1 mg/ml acridine for 15 mins. After incubation, cells were immediately analysed by flow cytometry. (E) Neurons (1×105) were stimulated with heme for indicated time, and were subjected to PI staining, and analyzed by flow cytometry. (F) Neurons were tranduced with DDIT3 RNAi or ATF4 RNAi for 24 hrs, and were further stimulated with control or heme for 6 hrs. Cells were subjected to PI staining, and analyzed by flow cytometry. Data are presented as the mean ± SD of three independent experiments. * P<0.05.

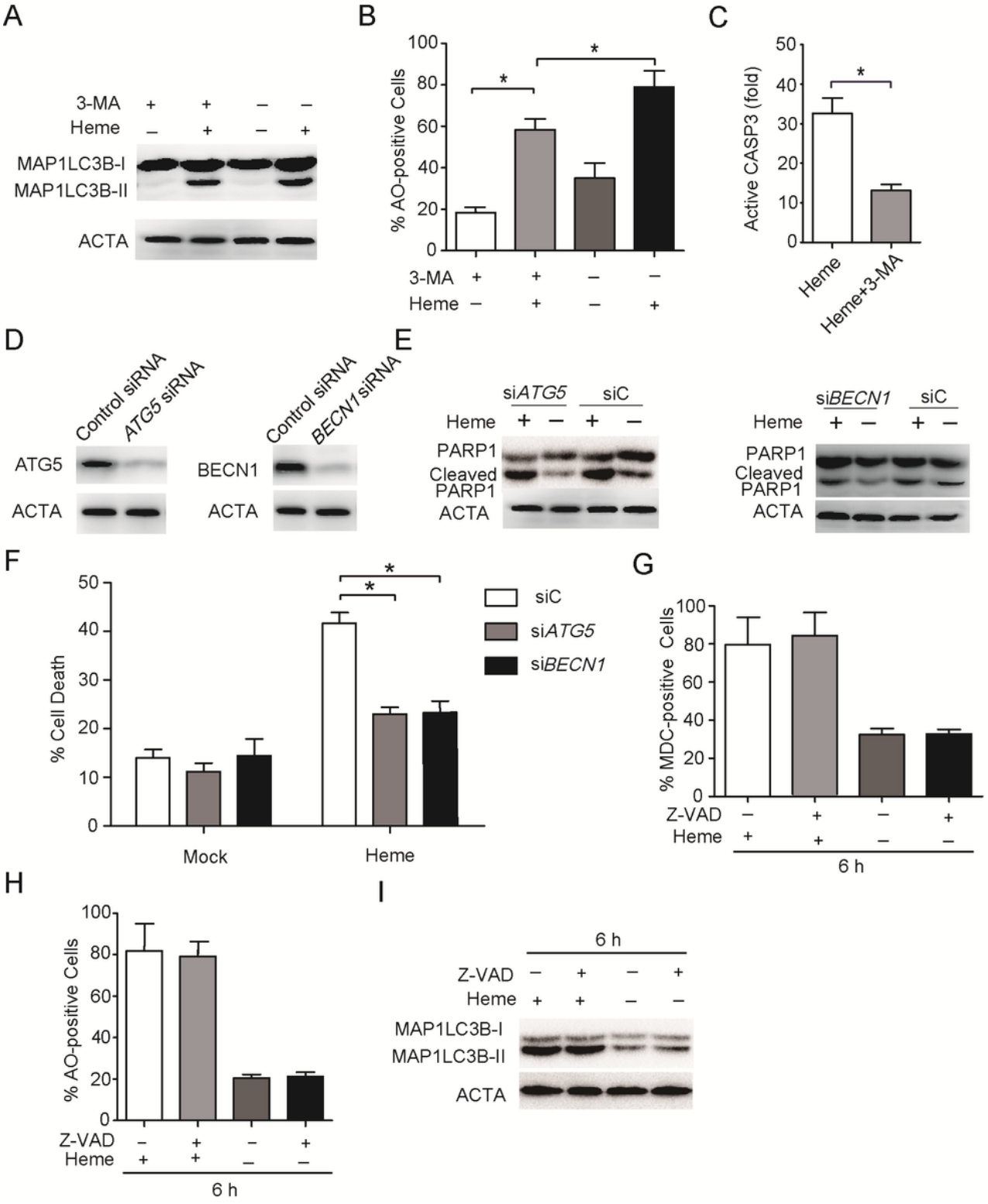

Figure 6

Autophagy is upstream of apoptosis in heme-induced cell death (A) Neurons (1×105) were stimulated with control, or heme in the presence or absence of 3-MA for 6 hrs, and MAP1LC3B-II levels were analyzed. (B) Neurons (1×105) were stimulated with control, or heme in the presence or absence of 3-MA for 6 hrs. Cells were stained with 1 mg/ml acridine orange for 15 mins. After incubation, cells were immediately analysed by flow cytometry. (C) Neurons (1×105) were stimulated with heme in the presence

or absence of 3-MA for 6 hrs. Cells were analyzed for 3-Caspase levels by Western blotting. (D) Detection of the inhibition efficiency of siRNAs against ATG5 and BECN1. Neurons were transfected with siRNAs targeting ATG5 or BECN1 (100 nM each) for 24 hrs, and the protein levels of the target were evaluated by Western blotting. (E) Neurons were tranduced with ATG5 RNAi or BECN1 RNAi for 24 hrs, and were further stimulated with control or heme for 6 hrs. Cells were analyzed for PARP1 levels by Western blotting. (F) Neurons were tranduced with ATG5 RNAi or BECN1 RNAi for 24 hrs, and were further stimulated with control or heme for 6 hs. Cells were subjected to PI staining, and analyzed by flow cytometry. (G-H) Neurons (1×105) were stimulated with control or heme in the presence or absence of Z-VAD for 6 hrs. Cells were stained with 50 mM MDC or 1 mg/ml acridine orange for 15 mins. After incubation, cells were immediately analysed by flow cytometry. (I) Neurons (1×105) were stimulated with control, or heme in the presence or absence of Z-VAD for 6 hrs, and MAP1LC3B-II levels were analyzed. Data are presented as the mean ± SD of three independent experiments. * $P<0.05$.